

Interactions in transversely isotropic new modified couple stress solid due to Hall current, rotation, inclined load with energy dissipation

Parveen Lata^a and Harpreet Kaur*

Department of Basic and Applied Sciences, Punjabi University, Patiala, Punjab, India

(Received August 22, 2023, Revised October 9, 2023, Accepted October 10, 2023)

Abstract. This paper is concerned with the disturbances in a transversely isotropic new modified couple stress homogeneous thermoelastic rotating medium under the combined influence of Hall currents, magnetic fields, and mechanical sources represented by inclined loads. The application of Laplace and Fourier transform techniques are used for the derivation of analytical expressions for various physical quantities. As an application, the bounding surface is subjected to uniformly and linearly distributed force (mechanical force). Present model contains length scale parameters that can capture the size effects. Numerical inversion techniques has been used to provide insights into the system's behavior in the physical domain. The graphical representation of numerical simulated results has been presented to emphasize the impact of rotation and inclined line loads on the system, enhancing our understanding of the studied phenomena. Further research can extend this study to investigate additional complexities and real-world applications.

Keywords: Hall current; inclined load; new modified couple stress; rotation; transversely isotropic

1. Introduction

A macro-scale analysis of materials can be made with the help of classical continuum mechanics theory, which ignores the microstructure size-dependency. For a more complete continuum theory, new deformation measures are needed. This implies that couple stresses must also be introduced into such a theory. Firstly, Voigt (1887) proposed the asymmetric theory of elasticity, and afterward in 1909, a couple stress theory was presented by Cosserat and Cosserat (1909), but examiners deemed the theory not important due to its failure to establishing the constitutive relations. Mindlin (1963) introduced a standard couple stress theory for isotropic materials with constitutive relation

$$\begin{aligned}\sigma_{ij} &= \lambda e_{kk} \delta_{ij} + 2G \varepsilon_{ij} \\ m_{ij} &= 4l^2 G \chi_{ij} \text{ where } \chi_{ij} = \omega_{i,j} \\ e_{ij} &= \frac{1}{2} (u_{i,j} + u_{j,i})\end{aligned}$$

*Corresponding author, Ph.D. Scholar, E-mail: mehrokpreet93@gmail.com

^aProfessor, E-mail: parveenlata@pbi.ac.in

$$\omega_i = \frac{1}{2} e_{ijk} u_{k,j}$$

Due to the asymmetric nature of the couple and curvature stress tensors, this theory is also designated as asymmetric couple stress theory. In addition, Koiter (1969) introduced constitutive relationships for anisotropic materials based on Cosserat couple stress theory.

$$\begin{aligned} \sigma_{ij} &= c_{ijkl} e_{kl} \\ m_{ij} &= l_i^2 G_i \chi_{ij}, l_i (i = 1, 2, 3) \text{ are length scale parameters} \end{aligned}$$

Employing the balance law for moments of couple besides the balance laws for forces and moment of forces a modified couple stress theory (M-CST) with one length scale parameter was offered by Yang *et al.* (2002). Application of this equilibrium equation leads to a symmetric couple-stress tensor. In M-CST

$$\begin{aligned} \chi_{ij} &= \frac{1}{2} (\omega_{i,j} + \omega_{j,i}), \\ \sigma_{ij} &= \lambda \varepsilon_{kk} \delta_{ij} + 2G \varepsilon_{ij} \\ m_{ij} &= 2l^2 G \widehat{\chi}_{ij} \end{aligned}$$

Chen *et al.* (2012) extended the modified couple stress theory to anisotropic elasticity namely new modified couple stress theory (newMCST) containing three length scale parameters. For newMCST,

$$\begin{aligned} \sigma_{ij} &= c_{ijkl} \varepsilon_{kl} \\ \chi_{ij} &= \omega_{i,j} \\ m_{ij} &= l_i^2 G_i \chi_{ij} + l_j^2 G_j \chi_{ji} \end{aligned}$$

Abbas (2007) studied the thermoelastic interactions in an infinite homogeneous elastic medium with a spherical or cylindrical cavity, using Green-Lindsay and Lord-Shulman theory. The cavity surface is subjected to a ramp-type heating of its internal boundary which is assumed to be traction free. The effect of rotation in generalized thermoelastic solid under the influence of gravity with an overlying infinite thermoelastic fluid was analyzed by Ailawalia and Narah (2009).

Kumar and Gupta (2010) investigated the deformation in an orthotropic micropolar thermoelastic solid with two relaxation times as a result of inclined load.

Large deflection thermoelastic analysis of functionally graded (FG) solid and hollow rotating axisymmetric disk with uniform and variable thickness subjected to thermo-mechanical loading is studied by Golmakani (2013), using first order shear deformation theory. Abouelregal and Zenkour (2013) used fractional order theory of thermoelasticity to study the effect of angular velocity on fiber-reinforced generalized thermoelastic medium whose surface is subjected to a Mode-I crack problem.⁷

Othman *et al.* (2014) considered the dual-phase lag model to study the influence of the rotation on a two-dimensional problem of micropolar thermoelastic isotropic medium with two temperatures. Zenkour and Abbas (2014) analyzed the nonlinear transient thermal stress conducted for temperature-dependent hollow cylinders subjected to a decaying-with-time thermal field Numerical results obtained with the assumptions of temperature-dependent and temperature-independent of the material properties are compared.

Sharma *et al.* (2015) investigated the two dimensional deformation in a homogeneous, transversely isotropic thermoelastic solids with two temperatures in context of Green-Naghdi theory of type-II as a result of an inclined load. Lou and He (2015) studied the nonlinear bending and free vibration responses of a simply supported functionally graded (FG) microplate lying on an elastic foundation within the context of the modified couple stress theory and the Kirchhoff/Mindlin plate

theory in combination with the von Karman's geometric nonlinearity.

Abbas and Kumar (2016) studied the plane problem in initially stressed thermoelastic half-space with voids due to thermal source. Lord-Shulman theory of thermoelasticity with one relaxation time has been used to investigate the problem. Dai and Dai (2016) studied the displacement and stress fields in a functionally graded material (FGM) hollow circular disk, rotating with an angular acceleration under a changing temperature field, by using a semi-analytical approach. Keivani *et al.* (2016) investigated the impacts of the vdW force and centrifugal force on the static behavior of the U-shaped and double sided nano-actuators. They applied the modified couple-stress theory (MCST) for deriving the governing equations and demonstrated that the vdW force decreases the external pull-in voltage of the system.

Kumar (2017) dealt with two dimensional problem in magneto-microstretch thermoelastic medium in the presence of combined effects of Hall current and rotation. The microstretch theory of thermoelasticity with two relaxation times derived by Eringen has been used to investigate the problem. Said *et al.* (2017) used normal mode technique to study thermodynamical interactions in amicropolar magneto-elastic medium with rotation and two-temperature. Abouelregal and Abo-Dahab (2018) researched a two-dimensional problem in the context of dual-phase-lag model with fiber-reinforcement and rotation using normal mode analysis.

Fard *et al.* (2018) studied the dynamical instability of three-layer micro-switch under DC voltage actuation using modified couple stress theory. Dynamic response of micro switch has been investigated with and without considering the damping effects. Ashraf (2018) presented a refined two-temperature multi-phase-lags thermoelasticity theory for the thermomechanical response of microbeams subjected to inclined load applying modified couple stress theory. Keivani *et al.* (2018) developed a mathematical model to study the effects of the electrostatic, Casimir and centrifugal forces on the static behaviors of the two U-shaped NEMS with rectangular and circular geometries. The size-dependent equations are obtained by employing the consistent couple stress theory (CCST). The D'Alembert principle is used to transform the angular speed into an equivalent static centrifugal force.

Rahi (2019) used the modified couple stress theory to capture size effect on dynamic behavior in a micro drill subjected to an axial load and a concentrated mass which is attached at its free end. Gunghas *et al.* (2019) investigated the two-dimensional deformations in a nonhomogeneous, isotropic, rotating, magneto-thermoelastic medium in the context of Green-Naghdi model III. Lata and Kaur (2019) dealt with the time harmonic interactions in transversely isotropic magneto thermoelastic solid with two temperatures (2T), rotation and without energy dissipation due to inclined load. Lord-Shulman theory has been formulated for this mathematical model. Lata and Harpreet (2019) studied the deformity in a homogeneous isotropic thermoelastic solid using modified couple stress theory subjected to inclined load with two temperatures with multi-dual-phase-lag heat transfer. Lata and kaur (2019) have considered transversely isotropic magneto thermoelastic solid with two temperature and without energy dissipation due to inclined load. The mathematical model has been formulated using Lord-Shulman theory. Size effective theories considered are modified couple stress theory (MCST), modified strain gradient theory (MSGT), nonlocal elasticity theory (NET), surface elasticity theory (SET), nonlocal surface elasticity theory (NSET). Kumar *et al.* (2019) studied the thermoelastic thin beam in a modified couple stress with three-phase-lag thermoelastic diffusion model subjected to thermal and chemical potential sources.

Abbas *et al.* (2020) investigated the photo-thermo-elastic interaction in an infinite semi-conductor material with cylindrical cavities loaded by a thermal shock varying heat. The effect of variable thermal conductivity through the photo-thermo-elastic transport process is studied using the

coupled models of thermo-elasticity and plasma waves. Alzahrani *et al.* (2020) investigated of a two-dimensional porous material under weak, strong and normal conductivity, using the eigenvalues method. Comparisons are made among the outcomes obtained under weak, normal and strong conductivity. Said (2020) investigated plane waves and the fundamental solution in rotating modified couple stress generalized thermoelastic solid with two-temperatures.

Hongwei *et al.* (2021) studied the amplitude motion and frequency simulation of a thick annular microsystem with graphene nanoplatelets (GPL) reinforcement in the framework of the modified couple stress theory (MCST). Marin *et al.* (2021) presented a model for porothermoelastic waves under a fractional time derivative and two times delays to study temperature increments, stress and the displacement components of the solid and fluid phases in porothermoelastic media. The governing equations are presented under Lord-Shulman theory with thermal relaxation time. Sharma *et al.* (2021) presented the rotating FGM disk with variable thickness by using finite element method (FEM). Thermo-elastic material properties and thickness of FGM disk continuously vary as exponential and power law function in radial direction along radius of disk. A comparative study of energy dissipation and quality factor evaluation in thin and thick beams pertaining to stress and strain conditions are done for diamond based microbeams by Resmi *et al.* (2021).

Based on the modified couple stress theory (MCST), the free vibration and buckling characteristics of porous functionally graded materials micro-beams (P-FGMs) are studied by Teng *et al.* (2022). Chang and Lee (2022) presented a general finite element formulation based on a six-field variational principle that incorporating the consistent couple stress theory. A simple, efficient and local iteration free solving procedure that covers both elastic and inelastic materials is derived to minimise computation cost. Esen (2022) presented a modified continuum mathematical model capable on investigation of dynamic behavior and response of perforated microbeam under the effect of moving mass/load based on modified couple stress theory and Timoshenko first-order shear beam theory.

Abouelregal *et al.* (2023) studied the effects of an axial heat supply on the thermomechanical behavior of an FG Piezoelectric thermally isolated rod using a modified Lord-Shulman model with the concept of a memory-dependent derivative (MDD). The exponential change of physical properties in the direction of the axis of the flexible rod is taken into account. It is assumed that there is no electric potential between the two ends of the rod.

The microstructure-dependent size effects have been exhibited by many micro- and nano-scale components and devices. Due to increase in the use of NEMS/MEMS transversely isotropic materials gain importance. And theories related to transversely isotropic media should be developed. Present model is capable to predict size effect at nano/macro scale. Rotating blades of wind mill are made up of fibre composites which show transversely isotropic properties. Water rotater is made up of timber, which is transversely isotropic. Nowadays pultruded Fiber Reinforced Polymer (FRP) thinwalled beams are usually employed in pedestrian bridges and bridge decks, as well as, more recently, in building structures. uniformly distributed load on the bridge deck an essential type of load that we must apply to the design. Also Bridge legs are build with the incline and decline. Titanium and its alloys are commonly used in the construction of aircraft due to its high strength properties, high-temperature resistance and high corrosion resistance. Also transversely isotropic aluminium is used in aircraft system. Thus present model a realistic model to study the deformation pattern in bridges and aircrafts, and also to capture size effects.

Objective of this paper is to study the homogeneous, new modifiedcouple stress thermoelastic medium medium under the combined effects of Hall currents, magnetic fields, and mechanical sources represented by inclined loads. The application of Laplace and Fourier transform techniques

are used for the derivation of analytical expressions for various physical quantities. As an application, the boundary surface is subjected to uniformly and linearly distributed force (mechanical forces). Numerical inversion techniques has been used to obtain the solution in the physical domain. The graphical representation of numerical simulated results has been presented to emphasize the effect of rotation and inclined line loads on the resulted quantities.

The advantage of use of integral transform technique is that manipulating and solving the equation is much easier in the transformed domain than in the original domain. The solution can then be mapped back to the original domain with the inverse of the integral transform.

2. Basic equations

Following Chen and Li (2012) and Devi (2017) the constitutive relations for a transversely isotropic new modified couple stress thermoelastic medium are given by

$$\sigma_{ij} = c_{ijkl}e_{kl} + \frac{1}{2}e_{ijk}m_{lk,l} - \beta_{ij}T, \quad (1)$$

Equation of motion for a transversely isotropic thermoelastic medium rotating uniformly with an angular velocity $\mathbf{\Omega} = \Omega n$, where n is a unit vector representing the direction of axis of rotation and taking into account Lorentz force

$$\sigma_{ij,j} + F_i = \rho \left\{ \ddot{u}_i + (\mathbf{\Omega} \times (\mathbf{\Omega} \times u))_i + (2\mathbf{\Omega} \times \dot{u})_i \right\}, \quad (2)$$

Following Chandrasekharaiah (1998) and Youssef (2007), The heat conduction equation with two temperature and with and without energy dissipation is given by

$$K_{ij}T_{,ij} + K_{ij}^*\dot{T}_{ij} = \beta_{ij}T_0\dot{e}_{ij} + \rho C_E\ddot{T}, \quad (3)$$

The above equations are supplemented by generalized Ohm's law for media with finite conductivity and including the Hall current effect

$$\mathbf{J} = \frac{\sigma_0}{1 + m^2} \left(\mathbf{E} + \mu_0 \left(\dot{\mathbf{u}} \times \mathbf{H} - \frac{1}{en_e} \mathbf{J} \times \mathbf{H}_0 \right) \right), \quad (4)$$

where

$$\beta_{ij} = c_{ijkl}\alpha_{ij}, \quad (5)$$

$$e_{ij} = \frac{1}{2}(u_{i,j} + u_{j,i}), \quad (6)$$

$$m_{ij} = l_i^2 G_i \chi_{ij} + l_j^2 G_j \chi_{ji}, \quad (7)$$

$$\chi_{ij} = \omega_{i,j}, \quad (8)$$

$$\omega_i = \frac{1}{2}e_{ijk}u_{k,j}. \quad (9)$$

Here

$$F_i = \mu_0(\mathbf{J} \times \mathbf{H}_0)_i, \text{ are the components of Lorentz force.}$$

$$\beta_{ij} = \beta_i \delta_{ij}, K_{ij} = K_i \delta_{ij}, K_{ij}^* = K_i^* \delta_{ij}, i \text{ is not summed}$$

Here $\mathbf{u} = (u_1, u_2, u_3)$ is the component of displacement vector, c_{ijkl} ($c_{ijkl} = c_{ijlk} = c_{jikl} = c_{jilk}$) are elastic parameters, σ_{ij} are the components of stress tensor, ε_{ij} are the components of strain tensor, e_{ijk} is alternate tensor, m_{ij} are the components of couple-stress, α_{ij} are the coefficients of linear thermal expansion, β_{ij} is thermal tensor, T is the temperature change, φ is the conductive temperature, l_i ($i = 1, 2, 3$) are material length scale parameters, χ_{ij} is curvature tensor, ω_i is the rotational vector, ρ is the density, K_{ij} is the materialistic constant, K_{ij}^* is the coefficient of thermal conductivity, c_E is the specific heat at constant strain, T_0 is the reference temperature assumed to be such that $T/T_0 \ll 1$, G_i are the elasticity constants, Ω is the angular velocity of the solid, H is the magnetic strength, $\dot{\mathbf{u}}$ is the velocity vector, \mathbf{E} is the intensity vector of the electric field, \mathbf{J} is the current density vector, $m (= \omega_e t_e = \frac{\sigma_0 \mu_0 H_0}{en_e})$ is the Hall parameter, t_e is the electron collision time, $\omega_e = \frac{e \mu_0 H_0}{m_e}$ is the electronic frequency, e is the charge of an electron, m_e is the mass of the electron, $\sigma_0 = \frac{e^2 t_e n_e}{m_e}$ is the electrical conductivity and n_e is the number of density of electrons.

3. Formulation and solution of the problem

We consider a homogeneous perfectly conducting transversely isotropic thermoelastic medium which is rotating uniformly with an angular velocity Ω initially at uniform temperature T_0 . The rectangular Cartesian co-ordinate system (u_1, u_2, u_3) having origin on the surface ($x_3=0$) with x_3 -axis pointing vertically downwards into the medium is introduced. The surface of the half-space is subjected to mechanical sources. For two dimensional problem in $x_1 x_3$ -plane, we take

$$\mathbf{u} = (u_1, 0, u_3). \quad (10)$$

We also assume that

$$\mathbf{E} = 0, \quad \Omega = (0, \Omega, 0). \quad (11)$$

The generalized Ohm's law

$$J_2 = 0. \quad (12)$$

The current density components J_1 and J_3 using (4) are given as

$$J_1 = \frac{\sigma_0 \mu_0 H_0}{1 + m^2} \left(m \frac{\partial u_1}{\partial t} - \frac{\partial u_3}{\partial t} \right), \quad (13)$$

$$J_3 = \frac{\sigma_0 \mu_0 H_0}{1 + m^2} \left(\frac{\partial u_1}{\partial t} + m \frac{\partial u_3}{\partial t} \right). \quad (14)$$

Following Slaughter (2002), using appropriate transformations, on the set of Eqs. (2) and (3) and with the aid of (5)-(10), we obtain the equations for transversely isotropic thermoelastic solid as

$$\begin{aligned} c_{11} \frac{\partial^2 u_1}{\partial x_1^2} + \left(c_{44} - \frac{1}{4} l_2^2 G_2 \nabla^2 \right) \frac{\partial^2 u_1}{\partial x_3^2} + \left(c_{13} + c_{44} + \frac{1}{4} l_2^2 G_2 \nabla^2 \right) \frac{\partial^2 u_3}{\partial x_1 \partial x_3} - \beta_1 \frac{\partial T}{\partial x_1} - \mu_0 J_3 H_0 \\ = \rho (\ddot{u}_1 - \Omega^2 u_1 + 2\Omega \dot{u}_3), \end{aligned} \quad (15)$$

$$\left(c_{44} + c_{13} + \frac{1}{4}l_2^2 G_2 \nabla^2\right) \frac{\partial^2 u_1}{\partial x_1 \partial x_3} + \left(c_{44} + \frac{1}{4}l_2^2 G_2 \nabla^2\right) \frac{\partial^2 u_3}{\partial x_1^2} + c_{33} \frac{\partial^2 u_3}{\partial x_3^2} - \beta_3 \frac{\partial T}{\partial x_3} + \mu_0 J_1 H_0 \quad (16)$$

$$= \rho(\ddot{u}_3 - \Omega^2 u_3 + 2\Omega \dot{u}_1),$$

$$\left(K_1 + K_1^* \frac{\partial}{\partial t}\right) \frac{\partial^2 T}{\partial x_1^2} + \left(K_3 + K_3^* \frac{\partial}{\partial t}\right) \frac{\partial^2 T}{\partial x_3^2} - \rho c_E \frac{\partial^2 T}{\partial t^2} = T_0 \frac{\partial}{\partial t} \left(\beta_1 \frac{\partial u_1}{\partial x_1} + \beta_3 \frac{\partial u_3}{\partial x_3}\right), \quad (17)$$

where $\nabla^2 = \left(\frac{\partial^2}{\partial x_1^2} + \frac{\partial^2}{\partial x_3^2}\right)$.

And the force stress constitutive relations, couple stress constitutive relations and strain components are

$$\sigma_{11} = c_{11} \frac{\partial u_1}{\partial x_1} + c_{13} \frac{\partial u_3}{\partial x_3} - \beta_1 T, \quad (18)$$

$$\sigma_{12} = 0, \quad (19)$$

$$\sigma_{13} = c_{44} \left(\frac{\partial u_1}{\partial x_3} + \frac{\partial u_3}{\partial x_1}\right) - \frac{1}{4}l_2^2 G_2 \left(\frac{\partial^3 u_1}{\partial x_1^2 \partial x_3} - \frac{\partial^3 u_3}{\partial x_1^3} + \frac{\partial^3 u_1}{\partial x_3^3} - \frac{\partial^3 u_3}{\partial x_3^2 \partial x_1}\right), \quad (20)$$

$$\sigma_{22} = c_{21} \frac{\partial u_1}{\partial x_1} + c_{23} \frac{\partial u_3}{\partial x_3} - \beta_1 T, \quad (21)$$

$$\sigma_{23} = 0, \quad (22)$$

$$\sigma_{33} = c_{31} \frac{\partial u_1}{\partial x_1} + c_{33} \frac{\partial u_3}{\partial x_3} - \beta_3 T, \quad (23)$$

$$m_{11} = 0, m_{22} = 0, m_{33} = 0, \quad (24)$$

$$m_{32} = \frac{1}{2}l_2^2 G_2 \left(\frac{\partial^2 u_1}{\partial x_3^2} - \frac{\partial^2 u_3}{\partial x_1 \partial x_3}\right), \quad (25)$$

$$m_{13} = 0, \quad (26)$$

$$m_{12} = -\frac{1}{2}l_2^2 G_2 \left(\frac{\partial^2 u_1}{\partial x_1 \partial x_3} - \frac{\partial^2 u_3}{\partial x_1^2}\right), \quad (27)$$

$$e_{11} = \frac{\partial u_1}{\partial x_1}, e_{22} = 0, e_{33} = \frac{\partial u_3}{\partial x_3}, e_{12} = 0, e_{23} = 0, e_{31} = \frac{1}{2} \left(\frac{\partial u_1}{\partial x_3} + \frac{\partial u_3}{\partial x_1}\right), \quad (28)$$

In the above equations we use the contracting subscript notations ($1 \rightarrow 11, 2 \rightarrow 22, 3 \rightarrow 33, 4 \rightarrow 23, 5 \rightarrow 31, 6 \rightarrow 12$) to relate c_{ijkl} to c_{mn}

We assume that medium is initially at rest. The undisturbed state is maintained at reference temperature. Then we have the initial and regularity conditions are given by

$$u_1(x_1, x_3, 0) = 0 = \dot{u}_1(x_1, x_3, 0),$$

$$u_3(x_1, x_3, 0) = 0 = \dot{u}_3(x_1, x_3, 0),$$

$$\begin{aligned} T(x_1, x_3, 0) = 0 = \dot{T}(x_1, x_3, 0) \text{ For } x_3 \geq 0, \quad -\infty < x_1 < \infty, \\ u_1(x_1, x_3, t) = u_3(x_1, x_3, t) = \varphi(x_1, x_3, t) = 0 \text{ for } t > 0 \text{ when } x_3 \rightarrow \infty. \end{aligned} \quad (29)$$

To facilitate the solution, following dimensionless quantities are introduced

$$\begin{aligned} x'_1 = \frac{x_1}{L}, x'_3 = \frac{x_3}{L}, u'_1 = \frac{\rho c_1^2}{L\beta_1 T_0} u_1, u'_3 = \frac{\rho c_1^2}{L\beta_1 T_0} u_3, T' = \frac{T}{T_0}, t' = \frac{c_1}{L} t, \sigma'_{ij} = \frac{\sigma_{ij}}{\beta_1 T_0}, \\ m'_{ij} = \frac{m_{ij}}{L\beta_1 T_0}, J' = \frac{\rho c_1^2}{\beta_1 T_0} J, h' = \frac{h}{H_0}, M = \frac{\sigma_0 \mu_0 H_0}{\rho c_1 L}, \Omega' = \frac{L}{c_1} \Omega. \end{aligned} \quad (30)$$

Using (29)-(30) on the Eqs. (15)-(17), yields

$$\begin{aligned} \frac{\partial^2 u_1}{\partial x_1^2} + \left(\delta_1 - \frac{1}{4L^2 c_{11}} l_2^2 G_2 \left(\frac{\partial^2}{\partial x_1^2} + \frac{\partial^2}{\partial x_3^2} \right) \right) \frac{\partial^2 u_1}{\partial x_3^2} + \left(\delta_2 + \frac{1}{4L^2 c_{11}} l_2^2 G_2 \left(\frac{\partial^2}{\partial x_1^2} + \frac{\partial^2}{\partial x_3^2} \right) \right) \frac{\partial^2 u_3}{\partial x_1 \partial x_3} - \\ \frac{Ms\mu_0 H_0}{(1+m^2)} (u_1 + mu_3) - \frac{\partial T}{\partial x_1} = \left(\frac{\partial^2 u_1}{\partial t^2} + \Omega^2 u_1 + 2\Omega \dot{u}_3 \right) \end{aligned} \quad (31)$$

$$\begin{aligned} \delta_4 \frac{\partial^2 u_3}{\partial x_3^2} + \left(\delta_2 + \frac{1}{4L^2 c_{11}} l_2^2 G_2 \left(\frac{\partial^2}{\partial x_1^2} + \frac{\partial^2}{\partial x_3^2} \right) \right) \frac{\partial^2 u_1}{\partial x_1 \partial x_3} + \left(\delta_1 - \frac{1}{4L^2 c_{11}} l_2^2 G_2 \left(\frac{\partial^2}{\partial x_1^2} + \frac{\partial^2}{\partial x_3^2} \right) \right) \frac{\partial^2 u_3}{\partial x_1^2} + \\ \frac{Ms\mu_0 H_0}{(1+m^2)} (mu_1 + u_3) - p_5 \frac{\partial T}{\partial x_3} = \left(\frac{\partial^2 u_3}{\partial t^2} - \Omega^2 u_3 + 2\Omega \dot{u}_1 \right) \end{aligned} \quad (32)$$

$$\frac{\partial^2 T}{\partial x_1^2} + p_3 \frac{\partial^2 T}{\partial x_3^2} = \zeta_1 L \frac{\partial^2 u_1}{\partial t \partial x_1} + \zeta_2 L \frac{\partial^2 u_3}{\partial t \partial x_3} + \zeta_3 \frac{\partial^2 T}{\partial t^2} \quad (33)$$

where

$$\begin{aligned} \delta_1 = \frac{c_{44}}{c_{11}}, \quad \delta_2 = \frac{c_{13} + c_{44}}{c_{11}}, \quad \delta_4 = \frac{c_{33}}{c_{11}}, \quad p_3 = \frac{K_3 + K_3^* s}{K_1 + K_1^* s}, \quad p_5 = \frac{\beta_3}{\beta_1}, \\ \zeta_1 = \frac{T_0 \beta_1^2}{(K_1 + K_1^* s) \rho}, \quad \zeta_2 = \frac{T_0 \beta_1 \beta_3}{(K_1 + K_1^* s) \rho}, \quad \zeta_3 = \frac{c_E c_{11}}{K_1 + K_1^* s}. \end{aligned}$$

Apply Laplace and Fourier transforms defined by

$$\bar{f}(x_1, x_3, s) = \int_0^\infty f(x_1, x_3, t) e^{-st} dt, \quad (34)$$

$$\hat{f}(\xi, x_3, s) = \int_{-\infty}^\infty \bar{f}(x_1, x_3, s) e^{i\xi x_1} dx_1. \quad (35)$$

on Eqs. (31)-(33), we obtain a system of homogeneous equations in terms of \bar{u}_1, \bar{u}_3 and \bar{T} which yield a non trivial solution if determinant of coefficient $\{\bar{u}_1, \bar{u}_3, \bar{T}\}^T$ vanishes and we obtain the following characteristic equation

$$(PD^8 + QD^6 + RD^4 + SD^2 + T)(\bar{u}_1, \bar{u}_3, \bar{T}) = 0, \quad (36)$$

where

$$P = -Ap_3\gamma_6 + \xi^2 A^2 p_3,$$

$$Q = -p_3\gamma_2\gamma_6 - A(-\gamma_5 p_3 + \gamma_6\gamma_9 + p_5\gamma_8) + \xi^2 A(-2p_3\gamma_4 + A\gamma_7),$$

$$R = -p_3\gamma_1\gamma_6 + \gamma_2(-\gamma_5p_3 + \gamma_6\gamma_9 + p_5\gamma_8) - A\gamma_5\gamma_9 - i\xi A(i\xi\gamma_4\gamma_9 + p_5\gamma_7) - \xi^2\gamma_4(-p_3\gamma_4 + A\gamma_7) + \xi^2A\gamma_8$$

$$S = -\gamma_1(-\gamma_5p_3 + \gamma_6\gamma_9 + p_5\gamma_8) + \gamma_2\gamma_5\gamma_9 - i\xi\gamma_4(i\xi\gamma_4\gamma_9 + p_5\gamma_7) - \gamma_3^2p_3 - i\xi(i\xi\gamma_4\gamma_8 - \gamma_6\gamma_7)$$

$$T = \gamma_1\gamma_5\gamma_9 - \gamma_3\gamma_9 + \gamma_5\gamma_9 + i\xi\gamma_5\gamma_7,$$

$$\gamma_1 = -(\xi^2 + s^2) - \frac{Ms\mu_0H_0}{(1+m^2)} + \Omega^2, \gamma_2 = \delta_1 + A\xi^2, \gamma_3 = \frac{Ms\mu_0H_0}{(1+m^2)} + 2\Omega s, \gamma_4 = \delta_2 - A\xi^2, \gamma_5 = -\xi^2\gamma_2 - \frac{Ms\mu_0H_0}{(1+m^2)} + \Omega^2 - s^2, \gamma_6 = \delta_4 - A\xi^2, \gamma_7 = i\xi\zeta_1Ls, \gamma_8 = \zeta_2Ls, \gamma_9 = \zeta_3s^2 - \xi^2.$$

The solution of the Eq. (36) satisfying the radiation condition that $\widehat{u}_1, \widehat{u}_3, \widehat{T} \rightarrow 0$ as $x_3 \rightarrow \infty$, can be written as

$$\widehat{u}_1 = A_1e^{-\lambda_1x_3} + A_2e^{-\lambda_2x_3} + A_3e^{-\lambda_3x_3} + A_4e^{-\lambda_4x_4}, \quad (37)$$

$$\widehat{u}_3 = R_1A_1e^{-\lambda_1x_3} + R_2A_2e^{-\lambda_2x_3} + R_3A_3e^{-\lambda_3x_3} + R_4A_4e^{-\lambda_4x_4}, \quad (38)$$

$$\widehat{T} = S_1A_1e^{-\lambda_1x_3} + S_2A_2e^{-\lambda_2x_3} + S_3A_3e^{-\lambda_3x_3} + S_4A_4e^{-\lambda_4x_4}. \quad (39)$$

where $\pm\lambda_i$, ($i=1,2,3$), are the roots of (36) and R_i and S_i are given as

$$R_i = \frac{p_3A\lambda_i^6 + (-\gamma_2p_3 - A\gamma_9)\lambda_i^4 + (-\gamma_1p_3 + \gamma_2\gamma_9)\lambda_i^2 + \gamma_1\gamma_9}{-\gamma_6p_3\lambda_i^4 + (-\gamma_5p_3 + \gamma_6\gamma_9)\lambda_i^2 + \gamma_5\gamma_9}$$

$$S_i = \frac{(-A\gamma_6 + \xi^2A^2)\lambda_i^6 + (-\gamma_2\gamma_6 - A\gamma_5 + 2\xi^2\gamma_4A)\lambda_i^4 + (\gamma_1\gamma_6 + \gamma_2\gamma_5 + \xi^2\gamma_4^2)\lambda_i^2 + (\gamma_1\gamma_5 - \gamma_3^2)}{-\gamma_6p_3\lambda_i^4 + (-\gamma_5p_3 + \gamma_6\gamma_9)\lambda_i^2 + \gamma_5\gamma_9}, \quad i = 1, 2, 3, 4.$$

4. Boundary conditions

We consider a normal line load F_1 per unit length acting in the positive x_3 axis on the plane boundary $x_3 = 0$ along the x_2 axis and a tangential load F_2 per unit length, acting at the origin in the positive x_1 axis. The boundary conditions are

$$t_{33}(x_1, x_3, t) = -F_1\psi_1(x_1)H(t), \quad (40)$$

$$t_{31}(x_1, x_3, t) = -F_2\psi_2(x_1)H(t), \quad (41)$$

$$m_{32}(x_1, x_3, t) = 0, \quad (42)$$

$$\frac{\partial T(x_1, x_3, t)}{\partial z} = 0. \quad (43)$$

where F_1 and F_2 are the magnitude of forces applied, $\psi_1(x_1)$ and $\psi_2(x_1)$ specify the vertical and horizontal load distribution functions respectively along x_1 -axis, $H(t)$ is the Heaviside unit step function (Fig. 1).

Substituting the values of $\widehat{u}_1, \widehat{u}_3, \widehat{T}$ from Eqs. (37)-(39) in the boundary conditions (40)-(43) and with the aid of (18)-(28), (30), (34)-(35) we obtain the components of displacement, thermodynamic temperature, components of stress and components of couple stress as

$$\tilde{u} = -\frac{F_1\widehat{\psi}_1(\xi)}{\Delta} \sum_{i=1}^4 B_{1i} e^{-\lambda_i x_3} - \frac{F_2\widehat{\psi}_2(\xi)}{\Delta} \sum_{i=1}^4 B_{2i} e^{-\lambda_i x_3}, \quad (44)$$

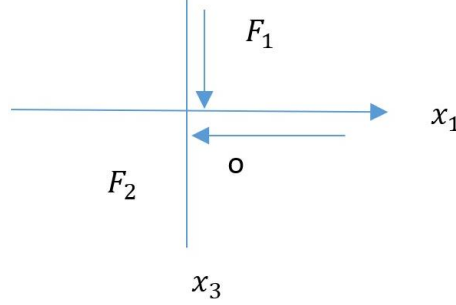


Fig. 1 Normal and tangential loadings

$$\tilde{w} = -\frac{F_1 \widehat{\psi}_1(\xi)}{\Delta} \sum_{i=1}^4 R_i B_{1i} e^{-\lambda_i x_3} - \frac{F_2 \widehat{\psi}_2(\xi)}{\Delta} \sum_{i=1}^4 R_i B_{2i} e^{-\lambda_i x_3}, \quad (45)$$

$$\tilde{T} = -\frac{F_1 \widehat{\psi}_1(\xi)}{\Delta} \sum_{i=1}^4 S_i B_{1i} e^{-\lambda_i x_3} - \frac{F_2 \widehat{\psi}_2(\xi)}{\Delta} \sum_{i=1}^4 S_i B_{2i} e^{-\lambda_i x_3}, \quad (46)$$

$$\widetilde{\sigma}_{33} = -\frac{F_1 \widehat{\psi}_1(\xi)}{\Delta} \sum_{i=1}^4 A_{1i} B_{1i} e^{-\lambda_i x_3} - \frac{F_2 \widehat{\psi}_2(\xi)}{\Delta} \sum_{i=1}^4 A_{1i} B_{2i} e^{-\lambda_i x_3}, \quad (47)$$

$$\widetilde{\sigma}_{31} = -\frac{F_1 \widehat{\psi}_1(\xi)}{\Delta} \sum_{i=1}^4 A_{2i} B_{1i} e^{-\lambda_i x_3} - \frac{F_2 \widehat{\psi}_2(\xi)}{\Delta} \sum_{i=1}^4 A_{2i} B_{2i} e^{-\lambda_i x_3}, \quad (48)$$

$$\widetilde{m}_{32} = -\frac{F_1 \widehat{\psi}_1(\xi)}{\Delta} \sum_{i=1}^4 A_{3i} B_{1i} e^{-\lambda_i x_3} - \frac{F_2 \widehat{\psi}_2(\xi)}{\Delta} \sum_{i=1}^4 A_{3i} B_{2i} e^{-\lambda_i x_3}. \quad (49)$$

$$\widehat{\sigma}_{11} = -\frac{1}{\Delta} \sum_{i=1}^4 \left(i\xi - \frac{c_{13}}{c_{11}} \lambda_i R_i - S_i \right) (F_1 \widehat{\psi}_1(\xi) B_{1i} + F_2 \widehat{\psi}_2(\xi) B_{2i}) e^{-\lambda_i x_3}, \quad (50)$$

$$\widehat{\sigma}_{22} = -\frac{1}{\Delta} \sum_{i=1}^4 \left(i\xi \frac{c_{21}}{c_{11}} - \frac{c_{13}}{c_{11}} \lambda_i R_i - S_i \right) (F_1 \widehat{\psi}_1(\xi) B_{1i} + F_2 \widehat{\psi}_2(\xi) B_{2i}) e^{-\lambda_i x_3}, \quad (51)$$

$$\widehat{m}_{12} = \frac{1}{2} \frac{\beta_1 T_0}{L^2 \rho c_1^2 \Delta} l_2^2 G_2 \sum_{i=1}^4 (-i\xi \lambda_i + \xi^2 R_i) (F_1 \widehat{\psi}_1(\xi) B_{1i} + F_2 \widehat{\psi}_2(\xi) B_{2i}) e^{-\lambda_i x_3}, \quad (52)$$

$$\tilde{J}_1 = \frac{c_1 \sigma_0 H_0 \mu_0 s}{(1+m^2)\Delta} \sum_{i=1}^4 (m - R_i) (F_1 \widehat{\psi}_1(\xi) B_{1i} + F_2 \widehat{\psi}_2(\xi) B_{2i}) e^{-\lambda_i x_3}, \quad (53)$$

$$\tilde{J}_3 = \frac{c_1 \sigma_0 H_0 \mu_0 s}{(1+m^2)\Delta} \sum_{i=1}^4 (1 + m R_i) (F_1 \widehat{\psi}_1(\xi) B_{1i} + F_2 \widehat{\psi}_2(\xi) B_{2i}) e^{-\lambda_i x_3}, \quad (54)$$

Where

$$\begin{aligned} A_{1i} &= \frac{i\xi c_{13}}{c_{11}} - \frac{c_{33}}{c_{11}} \lambda_i R_i - p_5 S_i, \\ A_{2i} &= \frac{c_{44}}{c_{11}} (-\lambda_i + i\xi R_i) - \frac{1}{4} \frac{\beta_1 T_0}{L^3 \rho c_1^2} l_2^2 G_2 \left((\xi^2 \lambda_i - \lambda_i^3) + (i\xi^3 - i\xi \lambda_i^2) R_i \right), \\ A_{3i} &= \frac{\beta_1 T_0}{2c_{11} L^2} l_2^2 G_2 (\lambda_i^2 + i\xi \lambda_i R_i), \end{aligned}$$

$$\begin{aligned}
A_{4i} &= -\lambda_i S_i, \\
\Delta &= \Delta_1 - \Delta_2 + \Delta_3 - \Delta_4, \\
\Delta_1 &= A_{11}A_{22}(A_{33}A_{44} - A_{43}A_{34}) - A_{11}A_{23}(A_{32}A_{44} - A_{42}A_{34}) + A_{11}A_{24}(A_{32}A_{43} - A_{42}A_{33}), \\
\Delta_2 &= A_{12}A_{21}(A_{33}A_{44} - A_{43}A_{34}) - A_{12}A_{23}(A_{31}A_{44} - A_{41}A_{34}) + A_{24}A_{12}(A_{31}A_{43} - A_{41}A_{33}), \\
\Delta_3 &= A_{13}A_{21}(A_{32}A_{44} - A_{42}A_{34}) - A_{22}A_{13}(A_{31}A_{44} - A_{41}A_{34}) + A_{13}A_{24}(A_{31}A_{42} - A_{41}A_{32}), \\
\Delta_4 &= A_{14}A_{21}(A_{32}A_{43} - A_{42}A_{33}) - A_{22}A_{14}(A_{31}A_{43} - A_{41}A_{33}) + A_{14}A_{23}(A_{31}A_{42} - A_{41}A_{32}), \\
B_{1i} &= (-1)^{1+i} \Delta_i / A_{1i}, \\
B_{21} &= -A_{21}(A_{33}A_{44} - A_{43}A_{34}) + A_{23}(A_{31}A_{44} - A_{41}A_{34}) - A_{24}(A_{31}A_{43} - A_{41}A_{33}), \\
B_{22} &= A_{11}(A_{33}A_{44} - A_{43}A_{34}) - A_{13}(A_{31}A_{44} - A_{41}A_{34}) + A_{14}(A_{31}A_{43} - A_{41}A_{33}), \\
B_{23} &= -A_{11}(A_{23}A_{44} - A_{43}A_{24}) + A_{13}(A_{21}A_{44} - A_{41}A_{24}) - A_{14}(A_{21}A_{43} - A_{41}A_{23}), \\
B_{24} &= A_{11}(A_{23}A_{34} - A_{33}A_{24}) - A_{13}(A_{21}A_{34} - A_{31}A_{24}) + A_{14}(A_{21}A_{33} - A_{31}A_{23}).
\end{aligned}$$

a) Influence function

The method to obtain the half-space influence function, i.e., the solution due to uniformly distributed force applied on the half space is obtained by setting

$$\{\psi_1(x_1), \psi_2(x_1)\} = \begin{cases} 1 & \text{if } |x| \leq m \\ 0 & \text{if } |x| > m \end{cases} \quad (55)$$

The Laplace and Fourier transforms of $\psi_1(x_1)$ with respect to the pair (x_1, ξ) for the case of a uniform strip load of non-dimensional width $2m$ applied at origin of co-ordinate system $x_1 = x_3 = 0$ in the dimensionless form after suppressing the primes becomes

$$\{\widehat{\psi}_1(\xi), \widehat{\psi}_2(\xi)\} = [2 \sin(\xi m) / \xi], \xi \neq 0. \quad (56)$$

The expressions for displacement components, stress components, conductive temperature and couple stress can be obtained for uniformly distributed normal force and thermal source by replacing $\widehat{\psi}_1(\xi)$ and $\widehat{\psi}_2(\xi)$ from (56) respectively in (44)-(54).

b) Linearly distributed Force

The solution due to linearly distributed force applied on the half space is obtained by setting

$$\{\psi_1(x_1), \psi_2(x_1)\} = \begin{cases} 1 - \frac{|x_1|}{m} & \text{if } |x| \leq m \\ 0 & \text{if } |x| > m \end{cases} \quad (57)$$

Here $2m$ is the width of the strip load, applying the Fourier transform defined by on (57), we obtain

$$\{\widehat{\psi}_1(\xi), \widehat{\psi}_2(\xi)\} = \left[\frac{2\{1 - \cos(\xi m)\}}{\xi^2 m} \right], \xi \neq 0. \quad (58)$$

Using (58) in the Eqs. (44)-(54), we obtain the components of displacement, stress, conductive temperature and components of couple stress.

Applications:

Inclined line load: Suppose an inclined load F_0 , per unit length is acting on the x_2 axis and its inclination with x_3 axis is δ , we have (see Fig. (b))

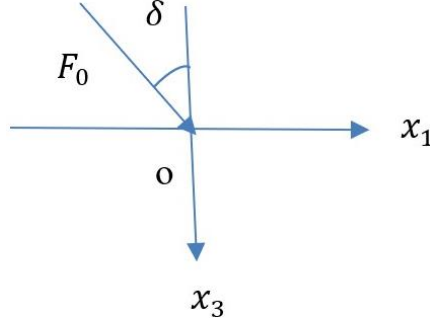


Fig. 2 Inclined load over a thermoelastic solid

$$F_1 = F_0 \cos \delta, \quad F_2 = F_0 \sin \delta. \quad (59)$$

5. Inversion of the transformations:

To obtain the solution of the problem in physical domain, we must invert the transforms in Eqs. (44)-(54). Here the displacement components, normal and tangential stresses and conductive temperature, couple stress are functions of x_3 , the parameters of Laplace and Fourier transforms s and ξ respectively and hence are of the form $f(\xi, x_3, s)$. To obtain the function $f(x_1, x_3, t)$ in the physical domain, we first invert the Fourier transform using

$$\bar{f}(x_1, x_3, t) = \frac{1}{2\pi} \int_{-\infty}^{\infty} e^{-i\xi x_1} \hat{f}(\xi, x_3, s) d\xi = \frac{1}{2\pi} \int_{-\infty}^{\infty} |\cos(\xi x_1) f_e - i \sin(\xi x_1) f_o| d\xi. \quad (60)$$

where f_e and f_o are respectively the odd and even parts of $\hat{f}(\xi, x_3, s)$. Thus the expression (60) gives the Laplace transform $\bar{f}(\xi, x_3, s)$ of the function $f(x, x_3, t)$. Following Honig and Hirdes (1984), the Laplace transform function $\bar{f}(\xi, x_3, s)$ can be inverted to $f(x_1, x_3, t)$.

The last step is to calculate the integral in Eq. (58). The method for evaluating this integral is described in Press *et al.* (1986). It involves the use of Romberg's integration with adaptive step size. This also uses the results from successive refinements of the extended trapezoidal rule followed by extrapolation of the results to the limit when the step size tends to zero.

6. Results and discussions

For the purpose of numerical evaluation, cobalt material has been chosen following Dhaliwal and Singh (1980) as

$c_{11} = 3.071 \times 10^{11} \text{ Nm}^{-2}$, $c_{12} = 1.650 \times 10^{11} \text{ Nm}^{-2}$, $c_{33} = 3.581 \times 10^{11} \text{ Nm}^{-2}$, $c_{13} = 1.027 \times 10^{11} \text{ Nm}^{-2}$, $c_{44} = 1.510 \times 10^{11} \text{ Nm}^{-2}$, $\rho = 8.836 \times 10^3 \text{ Kgm}^{-3}$, $T_0 = 298^\circ\text{K}$, $C_E = 4.27 \times 10^2 \text{ JKg}^{-1}\text{deg}^{-1}$, $K_1 = .690 \times 10^2 \text{ wm}^{-1}\text{deg}^{-1}$, $K_3 = .690 \times 10^2 \text{ wm}^{-1}\text{deg}^{-1}$, $\beta_1 = 7.04 \times 10^6 \text{ Nm}^{-2}\text{deg}^{-1}$, $\beta_3 = 6.90 \times 10^6 \text{ Nm}^{-2}\text{deg}^{-1}$, $K_1^* = 1 \times 10^2 \text{ Nsec}^{-2}\text{deg}^{-1}$, $K_3^* = 1 \times 10^2 \text{ Nsec}^{-2}\text{deg}^{-1}$, $\mu_0 = 1.2571 \times 10^{-6} \text{ Hm}^{-1}$, $H_0 = 1 \text{ Jm}^{-1}\text{nb}^{-1}$, $\varepsilon_0 = 8.838 \times 10^{-12} \text{ Fm}^{-1}$ with non-dimensional parameter $L=1$ and $\sigma_0 = 9.36 \times 10^5 \frac{\text{col}^2}{\text{Cal}}$. cm.sec, $t_0 = 0.01$, $M=3$, $F_0 = 1 \text{ N}$.

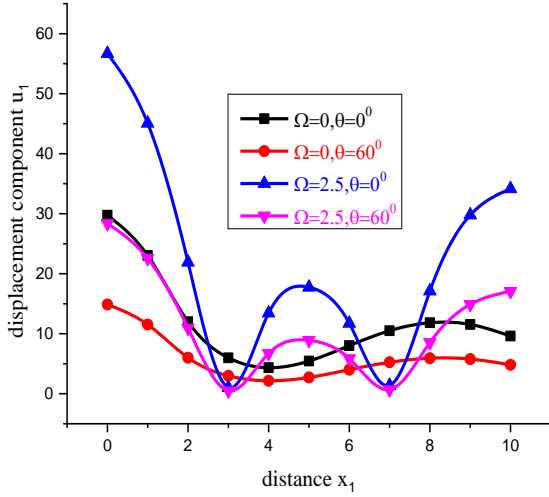


Fig. 3 Variation of displacement component u_1 with distance x_1 (uniformly distributed force)

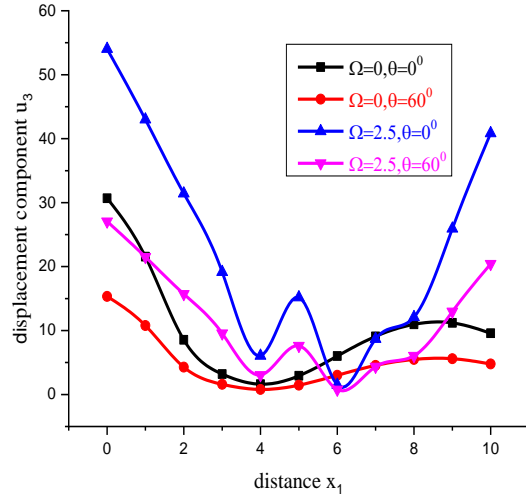


Fig. 4 Variation of displacement component u_3 with distance x_1 (uniformly distributed force)

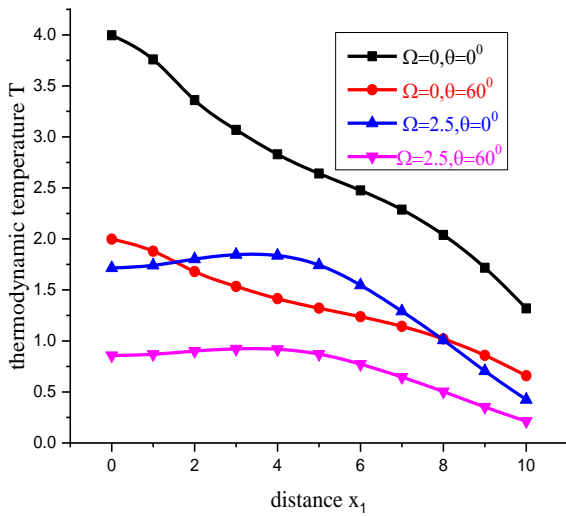


Fig. 5 Variation of thermodynamic temperature T with distance x_1 (uniformly distributed force)

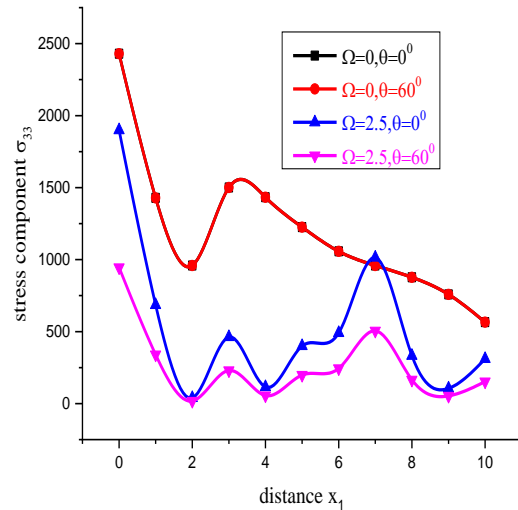


Fig. 6 Variation of stress component σ_{33} with distance x_1 (uniformly distributed force)

Using the above values the graphical representation of values of displacement components, thermodynamic temperature, stress components, couple stress components, transverse conduction current density J_1 and normal conduction current density J_3 for a transversely isotropic new modified couple stress have been investigated for uniformly distributed force and linearly distributed force to show a comparison of the effect of rotation and inclined load in the Figs. 3-24. The computations are carried out in the range $0 \leq x_1 \leq 10$.

Solid line in black with centre symbol square corresponds to $\Omega = 0, \theta = 0^0$, Solid line in red with centre symbol circle corresponds to $\Omega = 0, \theta = 60^0$, Solid line in blue with centre symbol

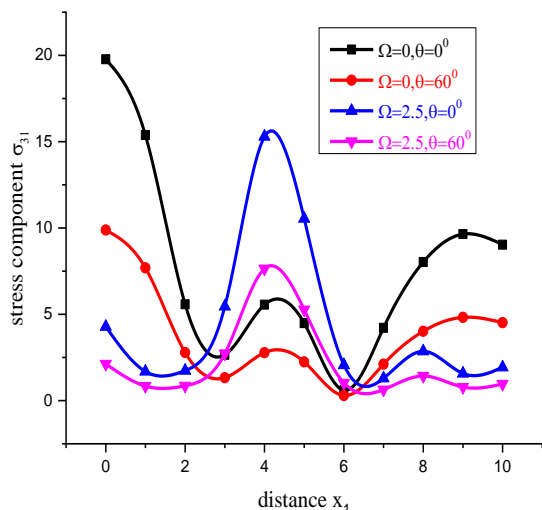


Fig. 7 Variation of stress component σ_{31} with distance x_1 (uniformly distributed force)

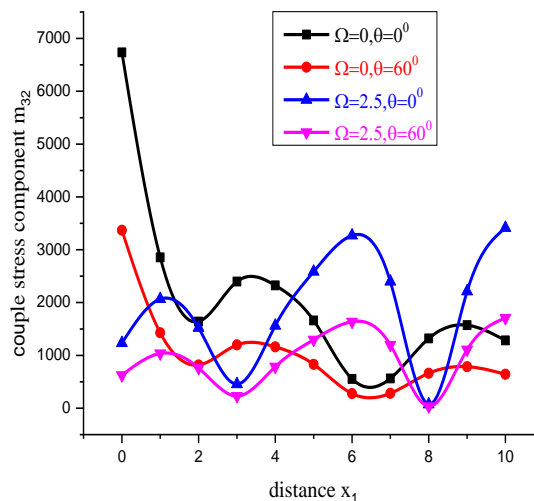


Fig. 8 Variation of couple stress component m_{12} with distance x_1 (uniformly distributed force)

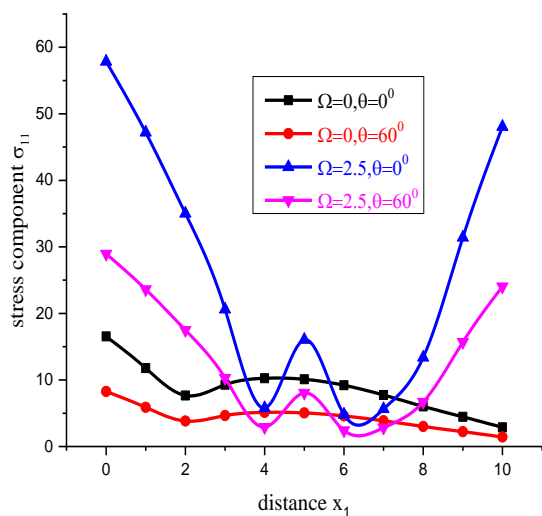


Fig. 9 Variation of stress component σ_{11} with distance x_1 (uniformly distributed force)

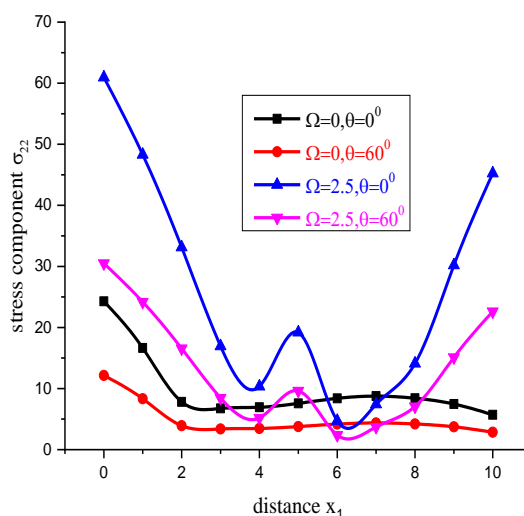


Fig. 10 Variation of stress component σ_{22} with distance x_1 (uniformly distributed force)

triangle corresponds to $\Omega = 2.5, \theta = 0^0$ and Solid line in magenta with centre symbol inverted tringle corresponds to $\Omega = 2.5, \theta = 60^0$.

Uniformly distributed force

In Figs. 3-4 curves depicting the variation of u_1 and u_3 are oscillatory in nature. Fluctuations are less for $\Omega = 0$ than the $\Omega = 2.5$. Inclination decreases the magnitude of quantity. In Fig. 5 variations for thermodynamic temperature T are smooth. In Figs. 6-8 variations for σ_{33}, σ_{31} and m_{32} are oscillatory. Inclination does not affect the σ_{33} for $\Omega = 0$. Rotation increases the oscillations

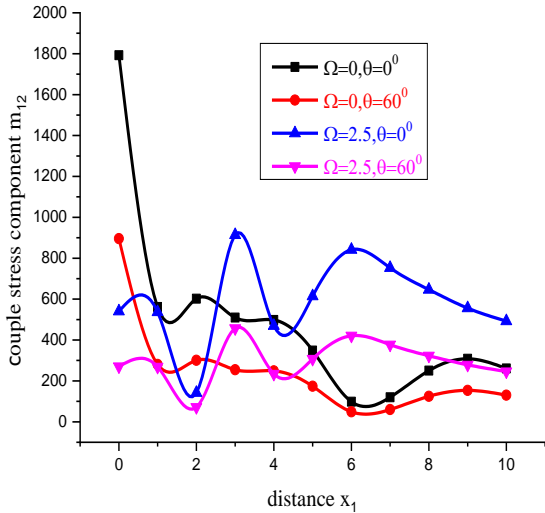


Fig. 11 Variation of couple stress component m_{12} with distance x_1 (uniformly distributed force)

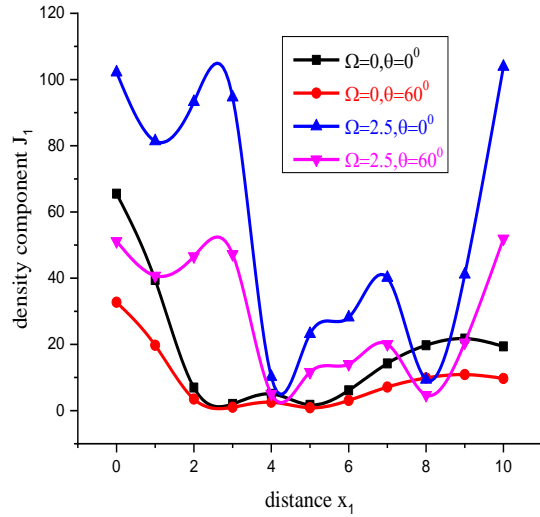


Fig. 12 Variation of transverse conduction current density J_1 with distance x_1 (uniformly distributed force)

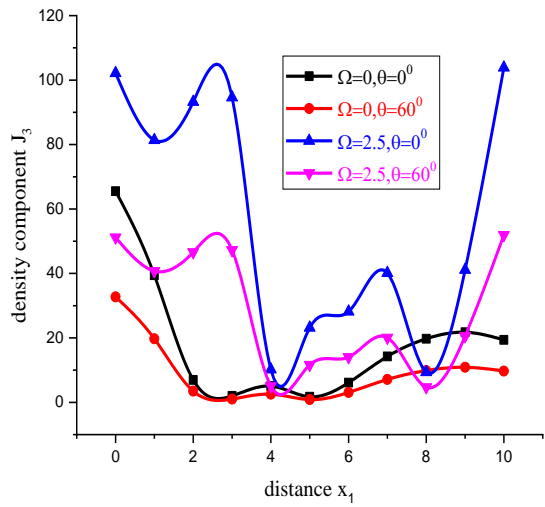


Fig. 13 Variation of normal conduction current density J_3 with distance x_1 (uniformly distributed force)

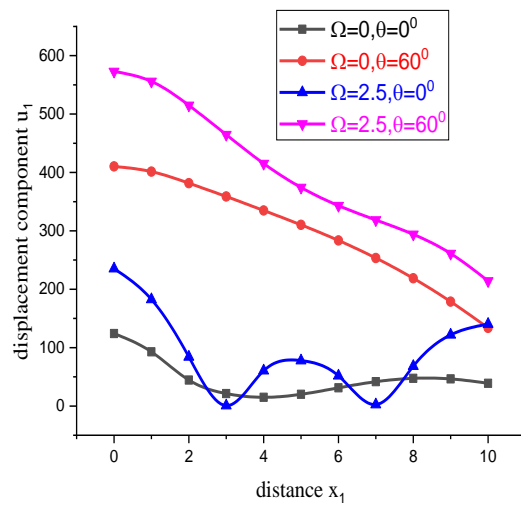


Fig. 14 Variation of displacement component u_1 with distance x_1 (linearly distributed force)

of σ_{33} . In Figs. 9-10 variations for σ_{11}, σ_{22} are *S* shape for $\Omega = 0$. For $\Omega = 2.5$ variations are oscillatory. In Figs. 11-13 variations corresponding to m_{12}, J_1 and J_3 are oscillatory in nature. Inclination changes the pattern of variation.

Linearly distributed force

In Figs. 14-15 for displacement components, for the given rotation inclined load decreases the amplitude and number of oscillations for the given horizontal range. In Fig. 16 T decreases with

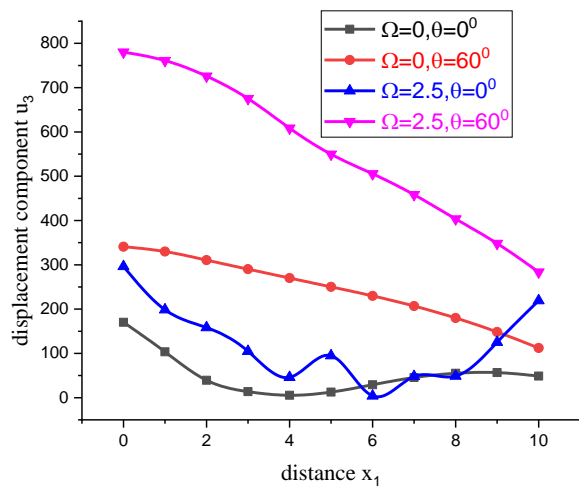


Fig. 15 Variation of displacement component u_3 with distance x_1 (linearly distributed force)

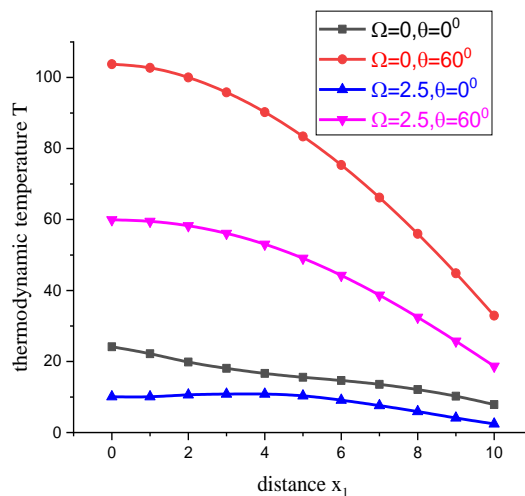


Fig. 16 Variation of thermodynamic temperature T with distance x_1 (linearly distributed force)

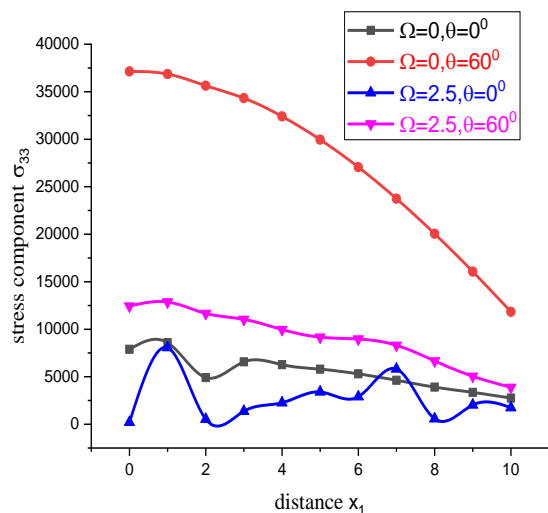


Fig. 17 Variation of stress component σ_{33} with distance x_1 (linearly distributed force)

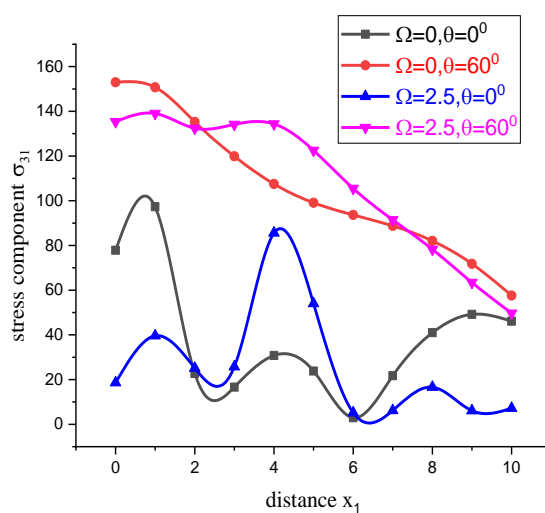


Fig. 18 Variation of stress component σ_{31} with distance x_1 (linearly distributed force)

increase in horizontal distance. In Fig. 17 σ_{33} for $\Omega = 0, \theta = 0^0$ decreases with increase in x_1 . In the remaining cases variations are oscillatory. In Figs. 18-19, σ_{31} and m_{32} shows oscillatory nature. Both rotation and inclination change the magnitude and pattern of variation. In Figs. 20-21, pattern for σ_{11} and σ_{22} is non-uniform. Maximum oscillations are seen for $\Omega = 2.5, \theta = 0^0$. For couple stress component m_{12} variations are oscillatory. In Figs. 20-21, pattern for J_1 and J_3 are similar to σ_{11} and σ_{22} .

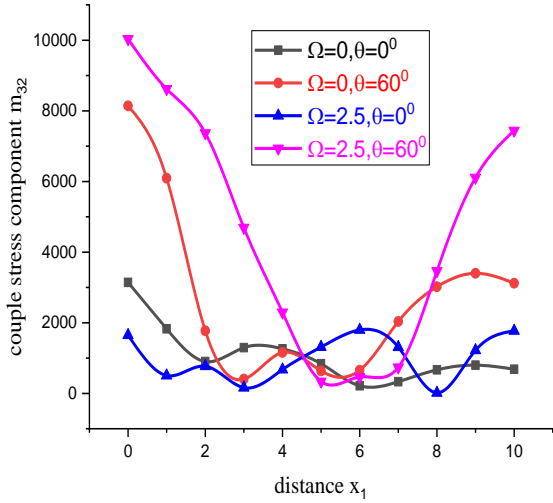


Fig. 19 Variation of couple stress component m_{32} with distance x_1 (linearly distributed force)

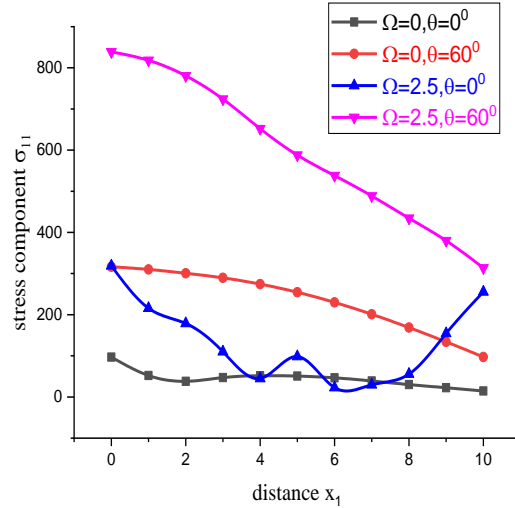


Fig. 20 Variation of stress component σ_{11} with distance x_1 (linearly distributed force)

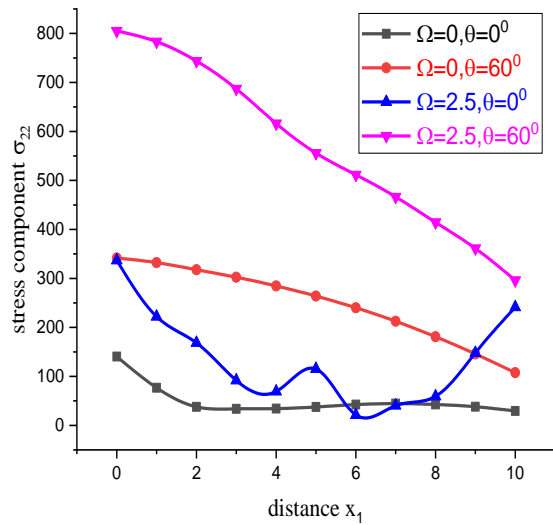


Fig. 21 Variation of stress component σ_{22} with distance x_1 (linearly distributed force)

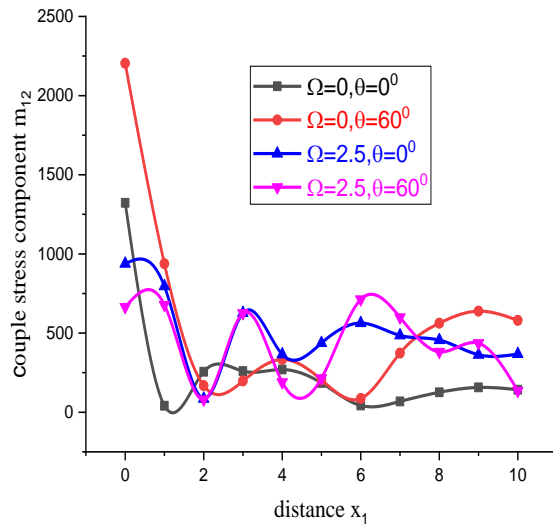


Fig. 22 Variation of couple stress component m_{12} with distance x_1 (linearly distributed force)

7. Conclusions

From the graphs, it is clear that inclined load and rotation have significant impacts on the resulting quantities. For uniformly distributed force and linearly distributed force inclination and rotation change the magnitude of oscillation. Inclusion of Inclined load decreases the magnitude of displacement components. Non uniform pattern of graphs is observed while applying linearly distributed mechanical force. σ_{11} and σ_{22} show maximum oscillations for $\Omega = 2.5, \theta = 0^0$. For linearly distributed force. For uniformly distributed source as the rotation changes pattern of

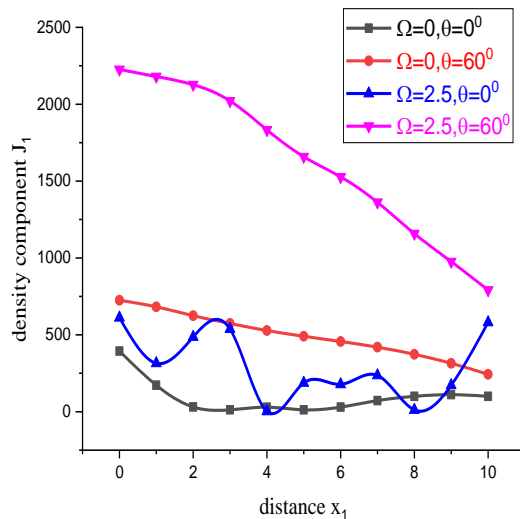


Fig. 23 Variation of transverse conduction current density J_1 with distance x_1 (linearly distributed force)

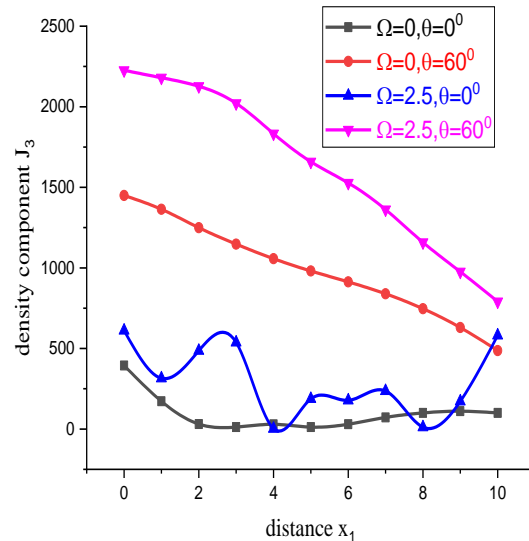


Fig. 24 Variation of normal conduction current density J_3 with distance x_1 (linearly distributed force)

oscillation also changes for σ_{11} and σ_{22} . Magnitude of current density components decreases as the inclination increases for uniformly distributed mechanical source. Reverse is observed in linearly distributed force. Rotation of principle axes and inclination of mechanical load changes the stress tensor. All the mentioned physical quantities are dependent upon rotation of principle axes and inclination of mechanical load. Consequently, varying rotation and inclination of mechanical load changes the pattern of deformation. Researchers working in thermomechanical sensors, resonators, medical accelerometers, as well as in future research, should benefit from the results of this research.

References

- Abaas, I.A. (2007), "Finite element analysis of the thermoelastic interactions in an unbounded body with a cavity", *Forsch Ingenieurwes*, **71**, 215-222. <https://doi.org/10.1007/s10010-007-0060-x>.
- Abbas, I.A. and Kumar, R. (2016), "2D deformation in initially stressed thermoelastic half-space with voids", *Steel Compos. Struct.*, **20**, 1103-1117. <https://doi.org/10.12989/scs.2016.20.5.1103>.
- Abbas, I.A., Hobiny, A. and Marin, M. (2020), "Photo-thermal interactions in a semi-conductor material with cylindrical cavities and variable thermal conductivity", *J. Taibah Univ. Sci.*, **14**(1), 1369-1376. <https://doi.org/10.1080/16583655.2020.1824465>.
- Abouelregal, A.E. and Abo-Dahab, S.M. (2018), "A two-dimensional problem of a mode-I crack in a rotating fibre-reinforced isotropic thermoelastic medium under dual-phase-lag model", *Sadhana*, **43**(1), 1-11. <https://doi.org/10.1007/s12046-017-0769-7>.
- Abouelregal, A.E. and Zenkour, A.M. (2013), "The effect of fractional thermoelasticity on a two-dimensional problem of a mode I crack in a rotating fiber-reinforced thermoelastic medium", *Chin. Phys. B*, **22**(1-8), 108102. <https://doi.org/10.1088/1674-1056/22/10/108102>.
- Abouelregal, A.E., Askar, S.S., Marin, M. and Mohamed, B. (2023), "The theory of thermoelasticity with a memory-dependent dynamic response for a thermo-piezoelectric functionally graded rotating rod", *Scientif.*

- Report.*, **13**, 9052. <https://doi.org/10.1038/s41598-023-36371-2>.
- Ailawalia, P. and Narah, N.S. (2009), "Effect of rotation in generalized thermoelastic solid under the influence of gravity with an overlying infinite thermoelastic fluid", *Appl. Math. Mech.*, **30**(12), 1505-1518. <https://doi.org/10.1007/s10483-009-1203-6>.
- Alzahrani, F., Hobiny, A., Abbas, I.A. and Marin, M. (2020), "An eigenvalues approach for a two-dimensional porous medium based upon weak, normal and strong thermal conductivities", *Symmetry*, **12**(5), 848. <https://doi.org/10.3390/sym12050848>.
- Chang, T.L. and Lee, C.L. (2022), "New mixed formulation and mesh dependency of finite elements based on the consistent couple stress theory", Preprint: arXiv:2207.02544v1.
- Chen, W., Xu, M. and Li, L. (2012), "A model of composite laminated Reddy plate based on new modified couple stress theory", *Compos. Struct.*, **94**(7), 2143-2156. <https://doi.org/10.1016/j.compstruct.2012.02.009>.
- Cosserat, E. and Cosserat, F. (1909), *Theory of Deformable Bodies*, Hermann et Fils, Paris.
- Dai, T. and Dai, H.L. (2016), "Thermo-elastic analysis of a functionally graded rotating hollow circular disk with variable thickness and angular speed", *Appl. Math. Model.*, **40**(17-18), 7689-7707. <https://doi.org/10.1016/j.apm.2016.03.025>.
- Esen, I., Abdelrahman, A.A. and Eltahir, M.A. (2022), "Dynamics analysis of Timoshenko perforated microbeams under moving loads", *Eng. Comput.*, **38**(3), 2413-242. <https://doi.org/10.1007/s00366-020-01212-7>.
- Fard, K.M., Gharechahi, A., Fard, N.M. and Mobki, H. (2018), "Investigation of dynamic instability of three plates switch under step DC voltage actuation using modified couple stress theory", *Lat. Am. J. Solid. Struct.*, **15**(7), 1-17. <https://doi.org/10.1590/1679-78254636>.
- Golmakani, M.E. (2013), "Large deflection thermoelastic analysis of shear deformable functionally graded variable thickness rotating disk", *Compos. Part B: Eng.*, **45**(1), 1143-1155. <https://doi.org/10.1016/j.compositesb.2012.08.012>.
- Gunghas, A., Kumar, R., Deswal, S. and Kalkal, K.K. (2019), "Influence of rotation and magnetic fields on a functionally graded thermoelastic solid subjected to a mechanical load", *J. Math.*, **2019**, Article ID 1016981. <https://doi.org/10.1155/2019/1016981>.
- Hongwei, L., Shen, S., Oslub, K., Habibi, M. and Safarpour, H. (2021), "Amplitude motion and frequency simulation of a composite viscoelastic microsystem within modified couple stress elasticity", *Eng. Comput.*, **38**(7), 3977-3991. <https://doi.org/10.1007/s00366-021-01316-8>.
- Honig, G. and Hirdes, U. (1984), "A method for the numerical inversion of the Laplace transform", *J. Comput. Appl. Math.*, **10**(1), 113-132. [https://doi.org/10.1016/0377-0427\(84\)90075-X](https://doi.org/10.1016/0377-0427(84)90075-X).
- Keivani, M., Gheisari, R., Kanani, A., Abadian, N., Mokhtari, J., Rach, R. and Abadyan, M. (2016), "Effect of the centrifugal force on the electromechanical instability of U-shaped and double-sided sensors made of cylindrical nanowires", *J. Brazil. Soc. Mech. Sci. Eng.*, **38**(7), 2129-2148. <https://doi.org/10.1007/s40430-016-0493-y>.
- Keivani, M., Mokhtari, J., Abadian, N., Abbasi, M., Koochi, A. and Abadyan, M. (2018), "Analysis of U-shaped NEMS in the presence of electrostatic, casimir, and centrifugal forces using consistent couple stress theory", *Iran. J. Sci. Technol. Trans. Sci.*, **42**, 1647-1658. <https://doi.org/10.1007/s40995-017-0151-y>.
- Koiter, W. (1964), "Couple-stresses in the theory of elasticity, I and II, Prec, Roy", *Netherlands Acad. Sci. B*, **67**, 0964.
- Kumar, A. (2017), "Elastodynamic effects of hall current with rotation in a microstretch thermoelastic solid", *Math./Stat.*, **20**(3), 345-354. <https://doi.org/10.6180/jase.2017.20.3.09>.
- Kumar, R. and Gupta, R.R. (2010), "Deformation due to inclined load in an orthotropic micropolar thermoelastic medium with two relaxation times", *Appl. Math. Inform. Sci.*, **4**(3), 413-428.
- Kumar, R., Devi, S. and Sharma, V. (2019), "Resonance of nanoscale beam due to various sources in modified couple stress thermoelastic diffusion with phase lags", *Mech. Mech. Eng.*, **23**(1), 36-49.
- Kumar, R., Sharma, K.D. and Garg, S.K. (2014), "Effect of two temperatures on reflection coefficient in micropolar thermoelastic with and without energy dissipation media", *Adv. Acoust. Vib.*, **2014**, Article ID 846721. <http://doi.org/10.1155/2014/846721>.

- Lata, P. and Kaur, H. (2021), "Deformation in a homogeneous isotropic thermoelastic solid with multi-dual-phase-lag heat & two temperature using modified couple stress theory", *Compos. Mater. Eng.*, **3**(2), 89-106. <https://doi.org/10.12989/cme.2021.3.2.089>.
- Lata, P. and Kaur, I. (2019), "Effect of inclined load on transversely isotropic magneto thermoelastic rotating solid with time harmonic source", *Adv. Mater. Res.*, **8**(2), 83-102. <https://doi.org/10.12989/amr.2019.8.2.083>.
- Lata, P. and Kaur, I. (2019), "Effect of rotation and inclined load on transversely isotropic magneto thermoelastic solid", *Struct. Eng. Mech.*, **70**(2), 245-255. <https://doi.org/10.12989/sem.2019.70.2.245>.
- Lou, J. and He, L. (2015), "Closed-form solutions for nonlinear bending and free vibration of functionally graded microplates based on the modified couple stress theory", *Compos. Struct.*, **131**, 810-820. <https://doi.org/10.1016/j.compstruct.2015.06.031>.
- Madić, M. and Radovanović, M. (2014), "Optimization of machining processes using pattern search algorithm", *Int. J. Indus. Eng. Comput.*, **5**(2), 223-234. <https://doi.org/10.5267/j.ijiec.2014.1.002>.
- Marin, M., Hobiny, H. and Abbas, I.A. (2021), "The effects of fractional time derivatives in porothermoelastic materials using finite element method", *Math.*, **9**(14), 1606. <https://doi.org/10.3390/math9141606>.
- Mindlin, R.D. (1963), "Influence of couple-stresses on stress concentrations", *Exp. Mech.*, **3**, 1-7. <https://doi.org/10.1007/bf02327219>.
- Othman, M.I.A., Hasona, W.M. and Abd-Elaziz, E.M. (2014), "Effect of rotation on micropolar generalized thermoelasticity with two temperatures using a dual-phase lag model", *Can. J. Phys.*, **92**(2), 149-158. <https://doi.org/10.1139/cjp-2013-0398>.
- Press, W.H., Teukolsky, S.A., Vetterling, W.T. and Flannery, B.P. (1986), *Numerical Recipes*, Cambridge University Press, Cambridge.
- Rahi, A. (2019), "Investigation into size effect on lateral vibrations of a micro-drill subjected to an axial load using the modified couple stress theory", *Scientia Iranica*, **26**(4), 2441-2453.
- Resmi, R., Babu, V.S. and Baiju, M.R. (2021), "Numerical study of thermoelastic damping effects on diamond based beams with plane stress and plane strain conditions applying nonclassical elasticity theory", *Adv. Dyn. Syst. Appl.*, **16**(2), 1371-1379.
- Said, S. (2020), "Fractional derivative heat transfer for rotating modified couple stress magneto-thermoelastic medium with two temperatures", *Wave. Random and Complex Media*, **32**(3), 1-18. <https://doi.org/10.1080/17455030.2020.1828663>.
- Said, S.M., Elmaklizi, Y.D. and Othman, M.I.A. (2017), "A two temperature rotating-micropolar thermoelastic medium under influence of magnetic field", *Chaos, Solit. Fract.*, **97**, 75-83. <https://doi.org/10.1016/j.chaos.2017.01.016>.
- Salem, A. (2018), "Refined two-temperature multi-phase-lags theory for thermomechanical response of microbeams using the modified couple stress analysis", *Acta Mechanica*, **229**(9), 3671-3692. <https://doi.org/10.1007/s00707-018-2172-9>.
- Sharma, D., Kaur, R. and Sharma, H., (2021), "Investigation of thermo-elastic characteristics in functionally graded rotating disk using finite element method", *Nonlin. Eng.*, **10**(1), 312-322. <https://doi.org/10.1515/nleng-2021-0025>.
- Sharma, N., Kumar, R. and Lata, P. (2015), "Disturbance due to inclined load in transversely isotropic thermoelastic medium with two temperatures and without energy dissipation", *Mater. Phys. Mech.*, **22**(2), 107-117.
- Slaughter, W.S. (2002), *The Linearised Theory of Elasticity*, Springer Science & Business Media, Birkhäuser Boston, Cambridge, U.S.A.
- Teng, Z., Wang, W. and Gu, C. (2022), "Free vibration and buckling characteristics of porous functionally graded materials (FGMs) micro-beams based on the modified couple stress theory", *Zeitschrift für Angewandte Mathematik und Mechanik*, **102**(4), e202100219. <https://doi.org/10.1002/zamm.202100219>.
- Voigt, W. (1887), "Theoretische studien über die elasticitätsverhältnisse der krystalle", Königliche Gesellschaft der Wissenschaften zu Göttingen.
- Yang, F., Chong, A.C.M., Lam, D.C.C. and Tong, P. (2002), "Couple stress based strain gradient theory for elasticity", *Int. J. Solid. Struct.*, **39**(10), 2731-2743. [https://doi.org/10.1016/S0020-7683\(02\)00152-X](https://doi.org/10.1016/S0020-7683(02)00152-X).

Zenkour, A. and Abbas, I.A. (2014), "Nonlinear transient thermal stress analysis of temperature-dependent hollow cylinders using a finite element mode", *Int. J. Struct. Stab. Dyn.*, **14**(6), 1450025. <https://doi.org/10.1142/S0219455414500254>.

CC